Changes in Photochemical Efficiency and Differential Induction of Superoxide Dismutase in Response to Combined Stresses of Chilling Temperature and Relatively High Irradiation in Two *Chlorella* Strains

Lee-Feng Chien and Wen-Hao Lin

Abstract

The green algae *Chlorella* sp. DT (DT) and *Chlorella pyrenoidosa* 211-8b (8b) had similar cell growth rates and photochemical efficiency (F_v/F_m) when they were cultivated under a moderate irradiance of 120 μmol photons $m^{-2} s^{-1}$ in combination with a series of temperatures that decreased from 32 to 7°C. Upon shifting the cultures to the relatively high irradiance of 240 μmol photons $m^{-2} s^{-1}$, DT exhibited higher cell growth rates than 8b under the chilling temperatures of 20°C and 15°C and differences in the F_v/F_m and Chl *a/b* ratios from 8b. In particular, DT possessed more new differentially induced SOD isoforms than 8b.

Keywords: *chlorella*, chilling temperature, relatively high irradiance, chlorophyll content, F_v/F_m, Chl *a/b*, superoxide dismutase

1. Introduction

The unicellular green alga *Chlorella* is a popular nutraceutical that is produced industrially in Taiwan. *Chlorella* requires a moderate climate, including ample sunshine and high temperatures of about 25–38°C for optimal large-scale outdoor growth. However, in winter, the temperature can range from 4 to 15°C, which is unsuitable for algal growth. In order to maintain productivity, it would be helpful to understand how green algae overcome chilling temperatures and a mimicking high irradiance resulted from chilling temperature [1–3].

Photosynthesis is the energy source for the growth and development of photosynthetic organisms. Photosynthetic efficiency is reliant on environmental conditions such as light and temperature. At low temperatures, algae experience reduced photosynthetic efficiency, whereas in high-light environments, they absorb more energy than they can consume in the photosynthetic processes [4]. The absorption of too much energy can lead to an increase in the production of reactive

oxygen species (ROS), which can damage the photosynthetic apparatus and further decrease photosynthetic efficiency [5]. Therefore, in response to wide daily and seasonal fluctuations in temperature and light, algae must possess some protective and regulatory systems to avoid this "energy excess" [6–9].

Upon initial exposure to low temperature or high irradiation, excessive excitation pressure may be induced between the rate of energy absorbed via the photosynthetic antenna and energy utilization [4, 5, 10–12]. One of the protection mechanisms that algae and higher plants employ to avoid receiving too much light energy is to adjust their chlorophyll (Chl) a/b ratios and the structure of the photosystem I and II (PSI and PSII) antenna complexes in response to different combinations of light intensity and temperature [2, 13–15]. Light-harvesting complexes (LHCs) with modified Chl composition have the ability to absorb different levels of light energy depending on the environmental conditions [16–18]. Another protective mechanism of algae and plants after receiving too much light energy is to adjust the antioxidant response of the scavenging system such that any excess excitation pressure is transferred to the superoxide radical ($O_2 \cdot ^-$) pathway and other derived reactive oxygen species (ROS) [19]. Superoxide dismutase (SOD, EC 1.15.1.1) is known as the first line of cellular defense against oxidative stress, and it catalyzes the dismutation of $O_2 \cdot ^-$ to H_2O_2 and O_2. There are three distinct types of SOD classified on the basis of their metal cofactors: the copper/zinc (CuZnSOD), iron (FeSOD), and manganese (MnSOD) isoenzymes [20]. SOD activity increases in cells in response to diverse environmental stresses including high light and chilling temperatures [21–23].

The primary objective of this present work was to explore combinations of light and temperature in algal cultures that may inform optimization of production system in manufacturing [24, 25]. The two warm-climate green algae, *Chlorella* sp. DT (DT) and *Chlorella pyrenoidosa* 211-8b (8b), were compared in their photosynthetic activity and antioxidant enzymatic responses under relatively high irradiance and various chilling temperatures [26, 27]. To determine the capacity of these algae to absorb light, their Chl contents and Chl a/b ratios were measured. Photochemical efficiency and the extent of photodamage were assessed by quantifying the chlorophyll fluorescence emission of PSII [28, 29]. The responses of SOD antioxidant enzymes to chilling and high-light acclimation were also examined because they enabled correlation with cell growth and photosynthetic activity [30].

2. Materials and methods

2.1 Chlorella culture and growing conditions

Chlorella sp. DT (DT) was discovered on the surface of power transmission cables near a mountain in central Taiwan, and *Chlorella pyrenoidosa* 211-8b (8b) was acquired from the Algal Collection Center at the University of Gottingen, Germany [26, 27]. Stock cultures were maintained at an initial concentration of 4 µg Chl mL^{-1} in 200 mL *Chlorella* medium in a 6 × 50 cm column at 32 ± 1°C in a water bath with continuous irradiance of 120 µmol photons m^{-2} s^{-1} and bubbling of 4% CO_2. In this study, six different temperatures and two different irradiance levels were used, but the growth conditions were similar.

2.2 Chlorophyll (Chl) determination

The growth of algal cultures was monitored by measuring the total Chl (Chl *a* + Chl *b*) content according to the method of Hoffman and Werner [28].

An algal culture of 5 mL was centrifuged for 5 min at 2000 × g (Sigma, MK-201, Germany). After the supernatant was removed, the algal cell pellet was collected, 5 mL of 100% methanol was added, and the mixture was heated at 60°C for 3 min. After centrifugation at 2000 × g for 10 min to remove any cell debris, the Chl extract was obtained. To determine the total Chl and Chl a/b ratios, the concentrations of Chl a and Chl b were measured spectrophotometrically according to Hoffman and Werner's equations:

$$\text{Chl } a \left(\mu\text{g mL}^{-1}\right) = 16.5 \times A_{665\text{nm}} - 8.3 \times A_{650\text{nm}}; \tag{1}$$

$$\text{Chl } b \left(\mu\text{g mL}^{-1}\right) = 33.8 \times A_{650\text{nm}} - 12.5 \times A_{665\text{nm}}; \tag{2}$$

$$\text{Total Chl } \left(\mu\text{g mL}^{-1}\right) = 4 \times A_{650\text{nm}} + 25.5 \times A_{665\text{nm}}. \tag{3}$$

The cell specific growth rate (μ, day^{-1}) was derived from the difference in cellular Chl content over time as follows:

$$\mu = \frac{\ln[\text{Chl}]_{t_2} - \ln[\text{Chl}]_{t_1}}{t_2 - t_1} \tag{4}$$

where $[\text{Chl}]t_1$ and $[\text{Chl}]t_2$ are the initial and final concentrations, at time t_1 and t_2, respectively.

2.3 Measurement of chlorophyll fluorescence parameters

Chlorophyll fluorescence was measured using a modulated chlorophyll fluorometer (Hansatech Instruments Ltd., Norfolk, UK). Algal samples were collected at the indicated times, adjusted to a concentration of 4 μg Chl mL^{-1}, and dark adapted for a period of 10 min at room temperature before measurement. The fiber-optic probe of the fluorometer was then placed into the chamber with 2 mL of the algal samples. The minimum fluorescence (F_0) with all open PSII reaction centers was determined by a weak non-actinic modulated light (<0.1 μmol m^{-2} s^{-1}). The maximum fluorescence (F_m) with all closed PSII reaction centers was induced by a saturating pulse of white light (1 s, 13,000 μmol m^{-2} s^{-1}) and measured after applying the actinic light (300 μmol m^{-2} s^{-1}). The variable fluorescence (F_v) was calculated as F_m-F_o, and the ratio of the variable to maximum fluorescence (F_v/F_m) represented the maximal photochemical efficiency [29, 30].

2.4 Spectrophotometrical assay of SOD activity

Algal cells from the log phase were collected by centrifugation. The cell pellet was washed three times and resuspended with extraction buffer (100 mM K_2PO_4 and 5 mM EDTA, pH 7.0). Algal cells were then broken down by sonication (V500, SONIC, USA) and centrifuged at 10,000 × g (MK-201, Sigma, Germany) for 15 min. The supernatant obtained was the algal crude extract. Protein concentrations of algal crude extracts were determined by the method of Lowry et al. [31] using BSA as the standard. The algal crude extracts were then subjected to a SOD assay.

The activity of the SODs was determined by measuring the inhibited reduction of cytochrome c (cyt c) because the SOD competed with cyt c for superoxide radicals, thus inhibiting cyt c reduction [32]. The reduction of cyt c was measured by monitoring the change in absorbance at 549 nm (cyt c absorption) when xanthine oxidase was added to a reaction mixture of K_2PO_4 (pH 7.8), xanthine, and

cyt c (oxidized) at room temperature. After a few seconds, the algal crude extract was added to the reaction mixture. SOD activity was then calculated as 50% of the inhibited reduction rate of cyt c. An extinction coefficient of ε_{549nm} = 21 mM^{-1} cm^{-1} for cyt c was used.

2.5 Native PAGE analysis of SOD

About 5–20 μg of protein from algal cell crude extracts suspended in sample buffer comprising 12.5 mM Tris–HCl (pH 6.8), 0.02% (w/v) bromophenol blue, and 4% (v/v) glycerol was loaded into each well. SODs in the algal extract were separated by native polyacrylamide gel electrophoresis (native PAGE) (10%). After electrophoresis the gels were washed with 100 mM K_2PO_4 buffer (pH 7.8) for 10 min and incubated in staining buffer composed of 20 mM K_2PO_4 buffer (pH 7.0), 0.05 mM riboflavin, 0.1 mM nitroblue tetrazolium (NBT), and 0.2% (w/v) TEMED in the dark at room temperature for 30 min [33]. Then gels were washed twice with 100 mM K_2PO_4 butter (pH 7.8) and exposed to light until the development of color-less bands. The colorless bands on the purple-stained gel indicated the existence of SOD because the free radicals produced by riboflavin are removed by the SOD, and as a consequence the colorless oxidized NBT in the SOD band is not converted into its purple reduced form. The reaction was then stopped by immersing the gels in deionized water. The SOD isoenzymes were identified on the basis of their sensitiv-ity to KCN (5 mM) or H_2O_2 (10 mM), which were added into the staining buffer when required. MnSODs are resistant to both inhibitors, Cu/ZnSODs are sensitive to both inhibitors, and FeSODs are resistant to KCN but sensitive to H_2O_2.

3. Results

3.1 Enhanced inhibition of cell growth by a combined stress of doubled irradiance and chilling

The Chl content was monitored during acclimation because it represented not only the level of cell growth but also the capacity for light absorption [34]. Under a moderate irradiance of 120 μmol photons m^{-2} s^{-1} at 32°C (**Figure 1A**), the Chl content of DT algal culture increased with acclimation time. The DT culture exhibited a maximum specific growth rate of 2.2 μg Chl mL^{-1} day^{-1} and reached a stationary phase on Day 3 at a content of 92 μg Chl mL^{-1}. At 20°C, DT growth was inhibited on Day 1, but growth resumed at a slower rate than the control on Day 2. When the temperature was lowered to 15, 10, or 7°C, DT stopped growing and even showed negative growth rates; 15°C seemed to be a critical temperature at which no net growth was observed. Under a doubled irradiance of 240 μmol photons m^{-2} s^{-1} at 32°C (**Figure 1B**), DT cells exhibited a maximum specific growth rate of 2.7 μg Chl mL^{-1} day^{-1} and reached the stationary phase on Day 1 at a content of 70 μg Chl mL^{-1}. At 20°C, DT cells initially ceased growth under this doubled irradiance but resumed growth on Day 3. Transferring cultures to temperatures below 20°C pro-moted cell death, while the critical temperature for avoiding the negative growth rate now rose to 17°C, two degrees higher than for moderate irradiation.

A similar response was observed in 8b cells during acclimation at the various temperatures. The 8b exhibited maximum specific growth rates of 2.1 and 2.7 μg Chl mL^{-1} day^{-1} at 32°C on Day 1 under irradiance of 120 and 240 μmol photons m^{-2} s^{-1}, respectively, and reached the stationary phase at about 98 and 69 μg Chl mL^{-1} on Day 3 (**Figure 2A, B**). However, once moved to temperatures below 20°C
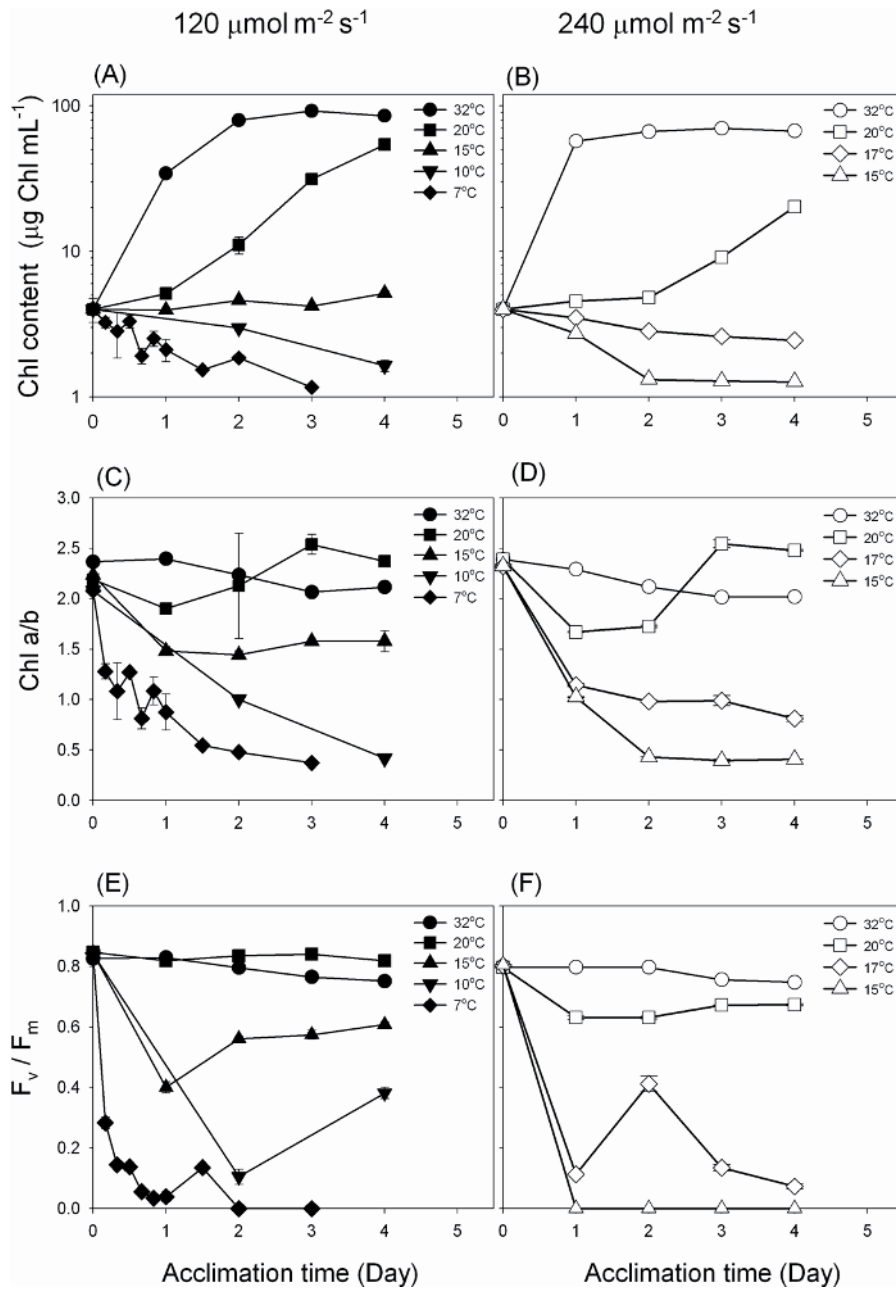
Figure 1.
Changes in the Chl content and photosynthetic activity of DT under irradiance of 120 or 240 μmol photons $m^{-2} s^{-1}$ during cultivation between 32 and 7°C. the total Chl content (A, B), the Chl a/b ratio (C, D), and the F_v/F_m ratio (E, F) of DT were measured each day. The initial cultivation concentration was 4 μg Chl mL^{-1}. Each point represents the mean ± SD (n = 4) from duplicate cultures (where not visible, error bars are smaller than the symbol).

under 240 μmol photons $m^{-2} s^{-1}$, the 8b culture after Day 3 produced slightly lower Chl content than DT after Day 3. For 8b, the critical temperatures below which no net cell growth occurred and cell death was observed under both 120 and 240 μmol photon $m^{-2} s^{-1}$ irradiance were 15°C and above 17°C, respectively.

Therefore, although a slightly higher maximum specific growth rate was observed initially at 32°C, lower temperatures induced enhanced inhibition of cell growth in both DT and 8b, and this was further inhibited under doubled irradiance.
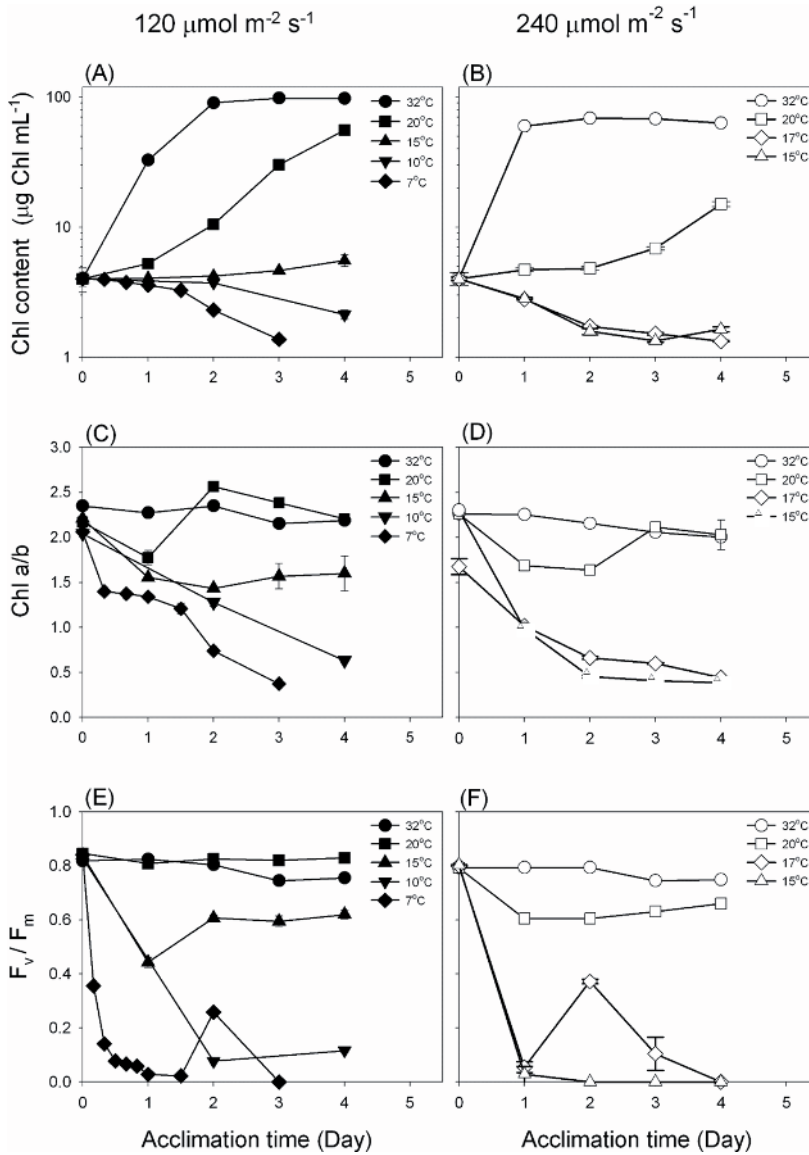
Figure 2.
Changes in the Chl content and photosynthetic activity of 8b under irradiance of 120 or 240 μmol photons
$m^{-2} s^{-1}$ during cultivation between 32 and 7°C. the total Chl content (A, B), the Chl a/b ratio (C, D), and the
F_v/F_m ratio (E, F) of 8b were measured each day. The initial cultivation concentration was 4 μg Chl mL^{-1}.
Each point represents the mean ± SD (n = 4) from duplicate cultures (where not visible, error bars are smaller
than the symbol).

3.2 The readjustment of Chl a/b ratios

In order to understand the influence of Chl composition on excitation energy transfer, the Chl *a/b* ratio was analyzed. Under 120 μmol photon $m^{-2} s^{-1}$ irradiance, the variation in the Chl *a/b* ratios of DT (**Figure 1C**) and 8b (**Figure 2C**) had similar trends at various temperatures. At 32°C, during acclimation, the Chl *a/b* ratios of both strains decreased slightly with time but remained between 2.4 and 2.1. When the cultures were moved to lower temperatures, the Chl *a/b* ratios changed dramatically. At 20°C, the Chl *a/b* ratios of both strains decreased to 1.7 by Day-1 but climbed back to about 2.1 by Day 2. At 15°C, the Chl *a/b* ratios of both strains were reduced to 1.0 on Day 1 and then remained at this value until the end of the experimental period. Under the lower temperatures of 10 and 7°C, the Chl *a/b* ratios of both strains rapidly declined to 0.4.

Under 240 μmol photon $m^{-2} s^{-1}$ irradiance, the Chl a/b ratios of DT (**Figure 1D**) and 8b (**Figure 2D**) acclimated to 32°C were similar to the ratios observed under 120 μmol photons $m^{-2} s^{-1}$. At lower temperatures, the Chl a/b ratios decreased with time, while it returned to a value of 2.6 on Day-3 and was higher than the value of 2.4 recorded for 8b.

3.3 Change in PSII photochemical efficiency

To assess the photochemical efficiency of PSII, the ratio of the variable to maximum fluorescence (F_v/F_m) was measured [28, 29]. In both algal cultures, the F_v/F_m ratios of the DT and 8b controls stayed initially in the 0.83–0.85 range at 32°C with an irradiance of 120 μmol photons $m^{-2} s^{-1}$, but decreased slightly to 0.74–0.75 by the end of the acclimation period (**Figures 1E, 2E**). The F_v/F_m ratios of both *Chlorella* strains were higher than those of most green algae but close to those of healthy green leaves of higher plants [28, 35–37]. This may be due to the antenna sizes of *Chlorella* PSII being different from those of other algae but similar to higher plants because the measured Chl fluorescence is assumed to originate from PSII [29, 38]. Algal cells grown at 20°C exhibited almost constant F_v/F_m ratios, which were similar to those at 32°C, although the cell growth rates were slower than those at 32°C. Once the cultures were transferred to 15°C, a significant decrease in the F_v/F_m ratios was observed, first falling to 0.40 for DT and 0.42 for 8b on Day 1 but by Day 2 recovering to 0.57 and 0.60 and staying at this value throughout the rest of the cultivation period. When the cultures were transferred to lower temperatures, the F_v/F_m ratios of DT and 8b fell rapidly to 0.08 and 0.10 at 10°C and 0.04 and 0.03 at 7°C, respectively, on Day 1 and continued to decrease to nearly zero by the end of the acclimation period.

Under 240 μmol photon $m^{-2} s^{-1}$ irradiance, at 32°C the F_v/F_m ratios of the DT and 8b strains also remained in 0.79–0.80 range (**Figures 1F, 2F**). However, the F_v/F_m ratios changed dramatically with lower temperatures. At 20°C, the F_v/F_m ratio of DT decreased to 0.20 on Day 2 but returned to 0.70 on Day 3, while in 8b it decreased to 0.40 but returned to 0.65 on Day 3. At 10 or 7°C, the F_v/F_m ratios of both strains declined to zero on Day 1, indicating that photosynthetic activity was immediately and completely inhibited. The Day 2 F_v/F_m ratios of both 8b and DT at 17°C and 7°C (**Figures 1E, F, 2E, F**) showed peaks that were probably due to experimental variations.

3.4 Shielding effects of high algal cell concentrations on light absorption

In order to understand whether the initial concentration of algal cells affected light absorption during chilling acclimation, cell growth was measured at different initial concentrations of 2, 4, and 6 μg Chl mL^{-1} under the doubled irradiance of 240 μmol photons $m^{-2} s^{-1}$.

By Day 3 following the initial cessation of growth at 20°C (**Figure 3A, B**), the DT and 8b cultures that started at concentrations of 4 and 6 μg Chl mL^{-1} were quicker to resume growth than those at 2 μg Chl mL^{-1} (**Figure 3A, B**). The Chl a/b ratios of DT decreased to 1.2, 1.7, and 2.0 with respect to initial concentrations of 2, 4, and 6 μg Chl mL^{-1} by Day 1, but then they increased close to control values by Day 3 (**Figure 3C**). The Chl a/b ratios of 8b showed similar variations with concentration to DT, with the exception of 2 μg Chl mL^{-1} (**Figure 3D**). The F_v/F_m ratios of DT and 8b initially decreased to 0.58 and 0.60 on Day-1; however, the ratios soon recovered and by Day-3 were 0.67 for DT and 0.63 for 8b (**Figure 3E, F**).

At 15°C, the cell growth of DT and 8b gradually declined with time regardless of the initial Chl concentrations. Nevertheless, at initial concentrations of 4 and 6 μg
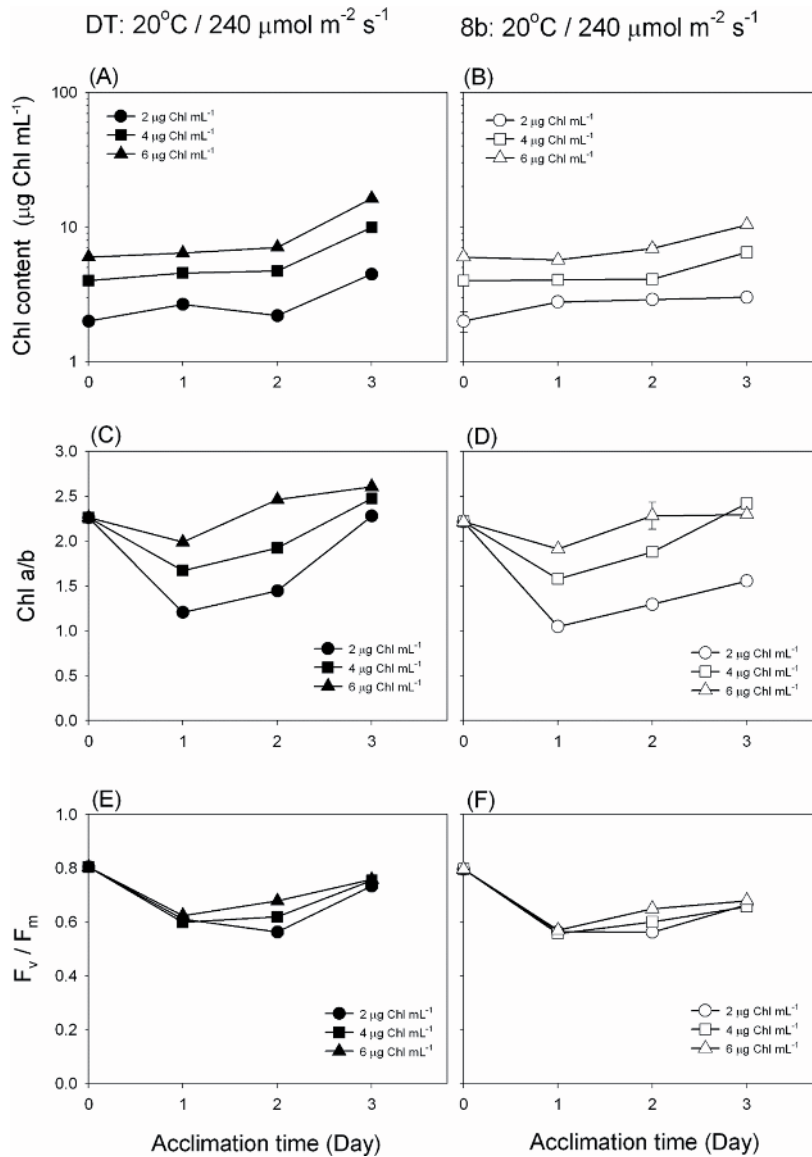
Figure 3.
Effect of initial cultivation concentration on photosynthesis under 20°C and 240 μmol photon m^{-2} s^{-1} irradiance. The total Chl content (A, B), the Chl a/b ratio (C, D), and the F$_v$/F$_m$ ratio (E, F) of Chlorella DT and 8b were measured in cultures with initial concentrations of 2, 4, and 6 μg Chl mL^{-1} at 20°C with irradiation of 240 μmol photons m^{-2} s^{-1}. Each point represents the average of two measurements from duplicate cultures (where not visible, error bars are smaller than the symbol).

Chl mL^{-1}, both strains were slower to die than cultures starting out at 2 μg Chl mL^{-1} (**Figure 4A, B**). Neither DT nor 8b at 2 μg Chl mL^{-1} resumed growth at 15°C, and no significant difference was recorded between the two strains. The Chl *a/b* ratios of DT and 8b (**Figure 4C, D**) rapidly decreased on Day 1 from 2.32 to 0.50, 1.03, and 1.65 with respect to the initial concentrations of 2, 4, and 6 μg Chl mL^{-1}, and no increases were observed for the duration of the acclimation period. The F$_v$/F$_m$ ratios of DT and 8b fell dramatically to near zero on Day 1 regardless of the initial concentrations, and no significant recovery was seen (**Figure 4E, F**).

The results suggested that the initial concentration (2, 4, and 6 μg Chl mL^{-1}) of algal cells did affect light absorption, but temperature was the major factor determining cell growth (**Figures 3, 4**). DT had a slightly greater tolerance at 20°C than 8b because its Chl a/b ratios attained levels higher than the control (Day 0), even though the Chl a/b ratios of 8b also returned to slightly above the control level.
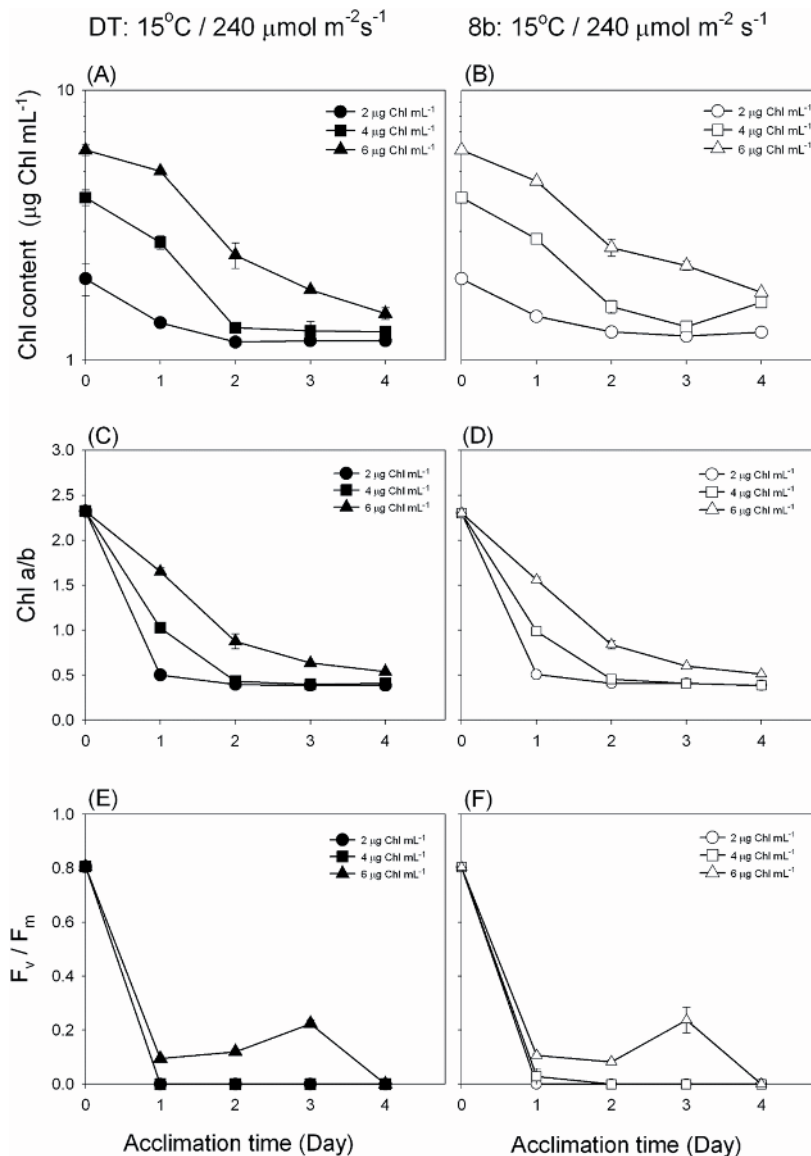
DT: 15°C / 240 μmol m^{-2}s^{-1}　　**8b: 15°C / 240 μmol m^{-2} s^{-1}**

Figure 4.
Effect of initial cultivation concentration on photosynthesis under 15°C and 240 μmol photon m^{-2} s^{-1} irradiance. The total Chl content (A, B), the Chl a/b ratio (C, D), and the F$_v$/F$_m$ ratio (E, F) of Chlorella DT and 8b were measured in the cultures with initial concentrations of 2, 4, and 6 μg Chl mL^{-1}. Each point represents the average of two measurements from duplicate cultures (where not visible, error bars are smaller than the symbol).

However, neither DT nor 8b could overcome the stress of low temperatures of 15°C and below combined with the doubled irradiance of 240 μmol photons m^{-2} s^{-1}.

3.5 Differential induction of multiple SOD isoforms

For the duration of the 15°C acclimation with 120 μmol photon m^{-2} s^{-1} irradiation, the specific growth rate of algal cells remained zero, implying that the energy input and output seemed to reach a critical point. To understand the contribution of antioxidants in scavenging ROS produced during chilling acclimation, the SOD activities were assayed with a spectrophotometrical method. It was found that DT had an approximately twofold higher rate of SOD activity (0.46 μmol mg^{-1} protein sec^{-1}) than 8b (0.21 μmol mg^{-1} protein sec^{-1}). Moreover, when the expression of SOD isoforms was examined after activity staining on native PAGE, three

distinct colorless bands were observed in DT (**Figure 5**) while only two bands were observed in 8b (**Figure 6**). The SOD activities of both strains were generally amplified with time and decreasing temperature. At the same time, some new SODs were induced, and some were diminished.

As shown in **Figure 5**, the DT control contained two DTMnSODs and three DTFeSODs, which were verified with inhibitors of H_2O_2 and KCN. Once the culture was moved to 15°C, the SOD activities of the DT increased greatly on Day-1 and reached a maximum on Day 2. By Day 4, at least 10 SOD isoforms were observed in DT including two new DTMnSODs and three new DTFeSODs. However, by Day 8, SOD activities declined, and some isoforms disappeared, leaving only three DTFeSODs and two DTMnSODs present. Similarly, as shown in **Figure 6**, the 8b control contained two 8bMnSODs and two 8bFeSODs. The SOD activities of 8b were amplified on Day 2 and reached a maximum on Day 4, while one new 8bMnSOD and two new 8bFeSODs were induced. At the end of acclimation, the SOD activity declined, and only two 8bFeSODs and two 8bMnSODs were present.
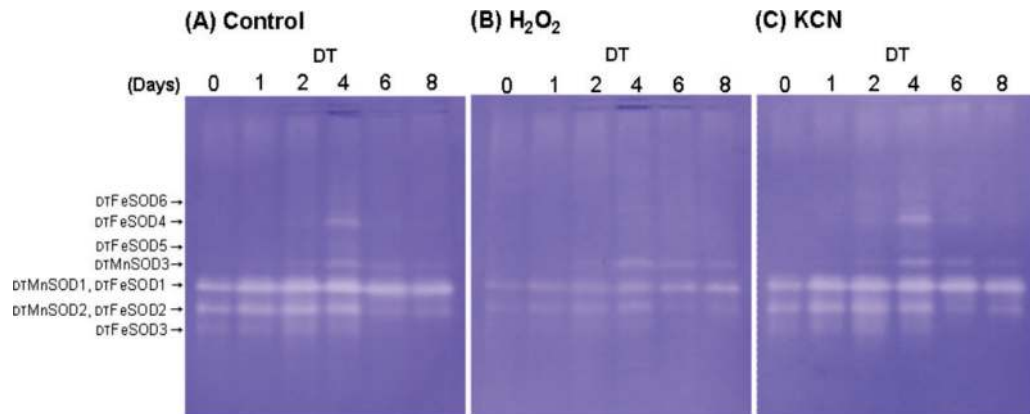

Figure 5.
Native PAGE analysis of SOD from a crude extract of DT grown at 15°C under 120 μmol photon $m^{-2} s^{-1}$ irradiance. In each well 5 μg of crude extract proteins was loaded. In comparison to the control (A), SOD isoforms were recognized by adding the inhibitors H_2O_2 (5 mM) (B) and 2 mM KCN (2 mM) (C). In total, nine SODs were induced differentially in DT with regard to six FeSODs and three MnSODs. The numbers represent the order of discovery.
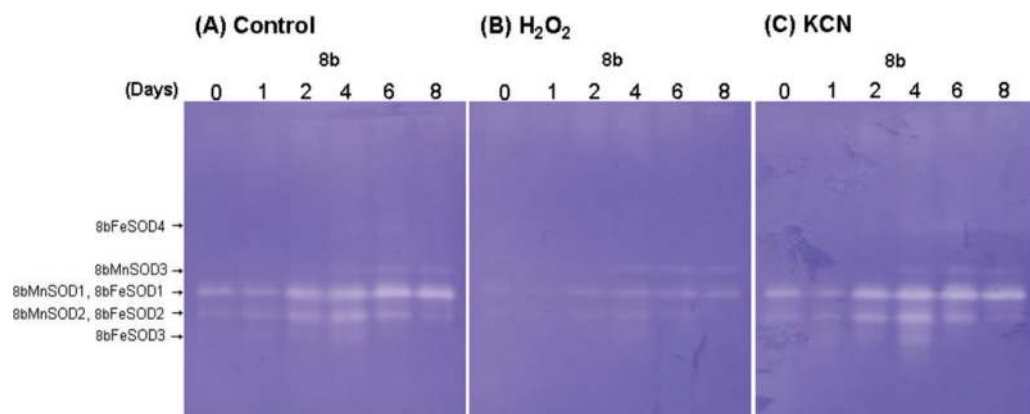
Figure 6.
Native PAGE analysis of SODs from crude extracts of 8b grown at 15°C under 120 μmol photon $m^{-2} s^{-1}$ irradiance. In each well 5 μg of crude extract proteins was loaded. In comparison to the control (A), SOD isoforms were recognized by adding the inhibitors H_2O_2 (5 mM) (B) and 2 mM KCN (2 mM) (C). Seven SODs were induced differentially in DT with regard to original four FeSODs and three MnSODs in 8b. The numbers represent the order of discovery.

These results suggest that DT and 8b utilize different strategies for scavenging $O_2 \cdot^-$. We found that MnSOD1 and FeSOD1 were the most abundant isoforms in both *Chlorella* strains, accounting for about 60–70% of the estimated total SOD activity. The other 30% is made up of other isoforms. The main FeSOD in both strains was particularly responsive to temperature [39]. Although there are three distinct types of SOD isoenzymes, only FeSOD and MnSOD were found in both *Chlorella* stains. Our observation of no CuZnSOD in either strain agrees with Asada et al. [40].

For further identification of which SOD isoforms responded to light stress and to temperature stress, the SODs were analyzed under lower temperature or doubled irradiance. In the DT culture, the original SOD isoforms of DTFeSOD1, DTFeSOD2, DTMnSOD1, and DTMnSOD2 were amplified in response to both the lower temperature of 10°C (**Figure 7A**) and to a doubled irradiance of 240 μmol photons $m^{-2} s^{-1}$ (**Figure 7B**). DTFeSOD3 disappeared on Day 1, probably because it was sensitive to both higher light and lower temperature. A newly induced DTFeSOD4 appeared on Day 1 in response to doubled irradiance, but it was not detected until

Figure 7.
Native PAGE analysis of SOD from crude extract of DT and 8b grown at 10°C under 120 μmol photon $m^{-2} s^{-1}$ irradiance (A) or 15°C under 240 μmol photon $m^{-2} s^{-1}$ irradiance (B). In (A), 15 μg of crude extract proteins was loaded in each well; in (B), 10 μg of crude extract proteins (except 1 μg proteins of DT on Day-2) was loaded. The numbers represent the order of discovery.

Day 1 under moderate irradiance, implying that DTFeSOD4 was probably more sensitive to light than to low temperatures. In 8b culture, in addition to the original SOD isoforms of 8bFeSOD1, 8bFeSOD2, 8bMnSOD1, and 8bMnSOD2, some new isoforms were induced. They were amplified in response to the lower temperature of 10°C (**Figure 7A**) and the doubled irradiance of 240 μmol photons $m^{-2} s^{-1}$ (**Figure 7B**) on Day 1. However, 8bMnSOD1 declined on Day 2. In spite of new SOD isoforms being amplified and in spite of the expectation that the SODs would prevent cell death, under the two combined stresses, the algal cells were still dying.

4. Discussion

4.1 Imbalance in excitation pressure

The specific growth rates on Day 1 from DT and 8b were plotted as a function of the cultivation temperatures (**Figure 8**). This showed that the specific growth rates decreased exponentially with decreasing temperatures from 32 to 10°C. Our results did not follow the previous observation of Sandnes et al. [41] where the specific growth rate of the green alga *Nannochloropsis oceanica* increased linearly with increasing low irradiance in the 17–26°C range. The curves fitted for the 120 μmol photon $m^{-2} s^{-1}$ irradiance data are dispersed from the 240 μmol photon $m^{-2} s^{-1}$ doubled irradiance data. Obviously, doubling the irradiance did not simply double the effect of the temperature reduction on the specific growth rate.

Furthermore, the relationship of specific growth rates versus cultivation temperatures was theoretically simulated in accordance with the excessive excitation pressure. The temperature coefficient (Q_{10}) represents the factor by which the speed of a biochemical reaction approximately doubles for every 10°C rise. Although some evidence indicated that Q_{10} in plants is temperature dependent [42], a Q_{10} of 2 was used here to theoretically estimate excessive excitation pressure. Therefore, the excessive excitation pressure due to the reduction in biochemical processes was calculated as $2^{(32°C-T_2)/10}$ (T, temperatures below 32°C) so that the theoretical excessive excitation pressure of
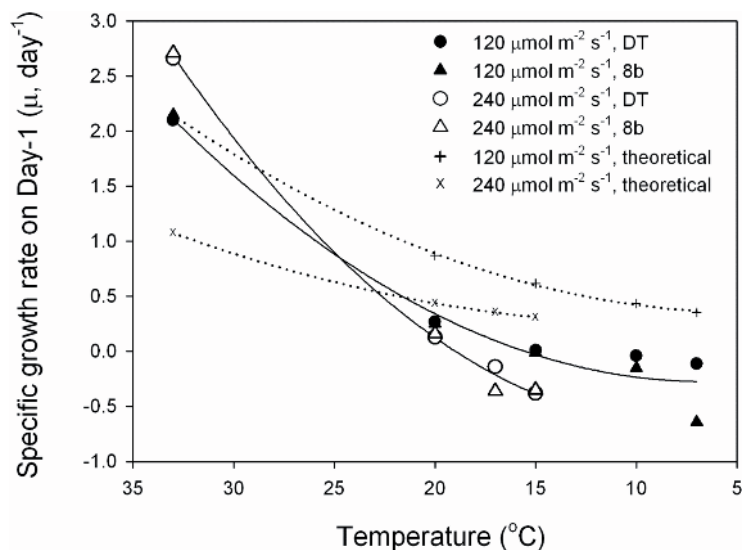

Figure 8.
Plots of measured and theoretical specific growth rates versus temperatures in DT and 8b. The solid line curves represent the measured specific growth rates at 120 (●, DT; ▲, 8b) and 240 (○, DT; Δ, 8b) μmol photon $m^{-2} s^{-1}$ irradiance. The dotted line curves represent theoretical specific growth rates at 120 (+) and 240 (×) μmol photon $m^{-2} s^{-1}$ irradiance.

Irradiation at 120 μmol photons m^{-2} s^{-1}

Temperature	Theoretical excessive excitation pressure (fold)	DT cell specific growth rate (μ) on Day-1 (μg Chl day^{-1})	8b cell specific growth rate (μ) on Day-1 (μg Chl day^{-1})
33°C	1-fold	2.15	2.07
20°C	2.5-fold	0.25	0.27
15°C	3.9-fold	−0.01	0.01
10°C	4.9-fold	−0.13	−0.04
7°C	6.1-fold	−0.69	−0.11

Irradiation at 240 μmol photons m^{-2} s^{-1}

Temperature	Theoretical excessive excitation pressure (fold)	DT cell specific growth rate (μ) on Day-1 (μg Chl day^{-1})	8b cell specific growth rate (μ) on Day-1 (μg Chl day^{-1})
33°C	2-fold	2.66	2.71
20°C	4.9-fold	0.13	0.16
17°C	6.1-fold	−0.14	−0.36
15°C	7.0-fold	−0.36	−0.35

Excessive excitation pressure was calculated upon the assumptions of temperature factor Q_{10} equaling to 2 for biochemical processes and light pressure factor equaling to 2 for double irradiance.

Table 1.
Theoretical excessive excitation pressure.

2.3-fold at 20°C, of 3.3-fold at 15°C, and so on were calculated relative to the control (onefold at 32°C) (**Table 1**). The diminished activities caused by theoretical excessive excitation pressure were plotted as a function of acclimation temperature (**Figure 8**). Subsequently, another plot was obtained for the doubled irradiance of 240 μmol photons m^{-2} s^{-1}, assuming that the excessive excitation pressure was twice the value under 120 μmol photon m^{-2} s^{-1} irradiance. However, the experimental curves did not follow the theoretical ones, implying that regulation of the response to the combined light and temperature stresses was more complicated than expected.

In our experiments, under a moderate irradiance of 120 μmol photons m^{-2} s^{-1}, DT and 8b showed no significant differences in growth rates and photochemical efficiency when subjected to various low temperatures. However, under a doubled irradiance of 240 μmol photons m^{-2} s^{-1}, DT had a slightly higher growth rate than 8b at temperatures below 20°C. This suggests that DT might possess a more efficient energy dissipation system against the combined stress of low temperatures and high irradiation than 8b. These results are in agreement with reports that the impact from photoinhibition due to low temperature and high light varies greatly across different green algal species [41, 43–45]. Although a greater specific growth rate was obtained under 240 μmol photon m^{-2} s^{-1} irradiance compared to 120 μmol photon m^{-2} s^{-1} irradiance, neither DT nor 8b favored high irradiance because a smaller Chl content was found during the stationary phase, that is, less biomass was generated.

In order to control light energy absorption and transfer, the LHC must modify the pigment composition of the Chl *a/b* ratio, and this is related to alterations in the photosynthetic apparatus under various conditions [16–18]. In the present study, decreases in both the Chl content and the Chl *a/b* ratio under low temperatures and high lights occurred simultaneously, suggesting a degradation of Chl molecules or the rearrangement of the LHCII complex [12]. A Chl *a/b* ratio of about 2.5 was obtained in both DT and 8b, which was similar to the green alga *Dunaliella salina* (2.3) [16], smaller than in *Chlorella vulgaris* (7.2) [2], and larger than in *Bryopsis maxima* (1.5) [38]. The lowering of Chl *a/b* ratios in DT and 8b is likely a mechanism to avoid absorbing too much light during acclimation [17]. The restoration of the Chl *a/b* ratio to 2.6 during 20°C acclimation might derive from the bleaching of Chl *b*, which is expected to absorb higher light excitation energy.

Despite the apparent decrease in the F_v/F_m ratios in our 10 and 7°C acclimation experiments, an initial increase and then a quenching of F_o was observed (data not shown). This phenomenon has been found in *C. vulgaris* and is suggested as being due to a rise in the xanthophyll cycle for dissipating excessive energy [43]. The reduction in both F_m and F_o implied changes in antenna size, thereby minimizing the absorbance of incident light [43]. Because F_o originates from the Chl *a* of the PSII-associated antenna, an increase in F_o is indicative of decreased energy transfer from LHCII to PSII. A large reduction in F_o has generally been regarded as a symptom of serious damage to the photosynthetic apparatus.

4.2 Differential SOD response

Since SOD is the first line of cellular defense against oxidative stress to remove $O_2 \cdot^-$, monitoring how SOD responds to photoinhibition during acclimation may provide more information about photoprotection [20]. It is known that SOD activity increases in cells in response to diverse environmental stresses including high light intensities and low temperatures and that SOD isoforms are expressed differently to protect against a subset of oxidative stresses under various environmental conditions [46, 47]. In particular, each of the SOD isoforms is independently regulated according to the degree of oxidative stress experienced in the respective subcellular compartments [48].

At 15°C acclimation and 120 µmol photon $m^{-2}\,s^{-1}$ irradiation, which was the point where the specific growth rate of the algal cells was zero, DT possessed higher SOD activities and more isoforms than 8b. To clarify further which SOD isoform responded to light or temperature, SOD activities were measured under the lower temperature conditions of 10°C and 120 µmol photon $m^{-2}\,s^{-1}$ irradiance (**Figure 7A**) and at 15°C under the doubled irradiance of 240 µmol photon $m^{-2}\,s^{-1}$ (**Figure 7B**). The results showed that the original SOD isoforms, which are likely sensitive to low temperature, were amplified by at 10°C and the newly induced SOD isoforms, which are likely sensitive to light, appeared under the doubled irradiance treatment.

Our data also suggested that the regulation of the antioxidant response to chilling was different from the response to irradiation. This raises the interesting question of why the regulation of antioxidant defenses is so highly complex and varied under a range of oxidative stresses even though they are targeting the same $O_2\cdot^{-}$ substrate [20–23].

5. Conclusion

The green algae *Chlorella* species DT (DT) and *Chlorella pyrenoidosa* 211-8b (8b) were very alike in their cell growth rate (total Chl), light energy absorption regulation (Chl *a/b* ratio), and photochemical efficiency (F_v/F_m) under optimal conditions of 120 µmol photons $m^{-2}\,s^{-1}$ and as temperatures decreased from 32 to 7°C. Upon exposure of the cultures to a doubled irradiance of 240 µmol photons $m^{-2}\,s^{-1}$, DT exhibited higher cell growth rates than 8b at chilling temperatures of 20°C and 15°C. It was also found that under the combined stresses of chilling temperature and relatively high irradiance, DT possessed higher SOD activity and more new SOD isoforms for removing free radicals than 8b.

Acknowledgements

Abbreviations

PS	photosystem
Chl	chlorophyll
F_m	maximum fluorescence
F_v	variable fluorescence
LHC	light-harvesting complex
SOD	superoxide dismutase
ROS	reactive oxygen species

Author details

Lee-Feng Chien* and Wen-Hao Lin
Department of Life Sciences, National Chung Hsing University, Taichung, Taiwan

*Address all correspondence to: lfchien@dragon.nchu.edu.tw

IntechOpen

References

[1] Allen DJ, Ort DR. Impact of chilling temperatures on photosynthesis in warm-climate plants. Trends in Plant Science. 2002;**6**:36-42

[2] Maxwell DP, Falk S, Trick CG, Hüner NP. Growth at low temperature mimics high-light acclimation in *Chlorella vulgaris*. Plant Physiology. 1994;**105**:535-543

[3] Singh SP, Singh P. Effect of temperature and light on the growth of algae species: A review. Renewable and Sustainable Energy Reviews. 2015;**50**:431-444

[4] Hüner NPA, Öquist G, Sarhan F. Energy balance and acclimation to light and cold. Trends in Plant Science. 1998;**3**:224-230

[5] Ort DR. When there is too much light. Plant Physiology. 2001;**125**:29-32

[6] Niyogi KK. Photoprotection revisited: Genetic and molecular approaches. Annual Review of Plant Physiology and Plant Molecular Biology. 1999;**50**:333-359

[7] Thomashow MF. Plant cold acclimation: Freezing tolerance genes and regulatory mechanisms. Annual Review of Plant Physiology and Plant Molecular Biology. 1999;**50**:571-599

[8] Mittler R. Oxidative stress, antioxidants and stress tolerance. Trends in Plant Science. 2002;7:405-410

[9] Suzuki N, Mittler R. Reactive oxygen species and temperature stresses: A delicate balance between signaling and destruction. Physiologia Plantarum. 2006;**126**:45-51

[10] Wilson KE, Ivanov AG, Öquist F, Grodzinski B, Sarhan F, Hüner NPA. Energy balance, organellar redox status, and acclimation to environmental stress. Canadian Journal of Biotany. 2006;**84**:1355-1370

[11] Guy C, Kaplan F, Kopka J, Selbig J, Hincha DH. Metabolomics of temperature stress. Physiologia Plantarum. 2008;**132**:220-235

[12] Takahashi S, Murata N. How do environmental stresses accelerate photoinhibition? Trends in Plant Science. 2008;**4**:178-182

[13] Wilson KE, Hüner NP. The role of growth rate, redox-state of the plastoquinone pool and the trans-thylakoid delta pH in photoacclimation of *Chlorella vulgaris* to growth irradiance and temperature. Planta. 2000;**212**:93-102

[14] Finazzi G, Minagawa J. High light acclimation in green microalgae. In: Demmig-Adams B, Garab G, Adams W III, Govindjee, editors. Non-Photochemical Quenching and Energy Dissipation in Plants, Algae and Cyanobacteria. Advances in Photosynthesis and Respiration (Including Bioenergy and Related Processes), Vol. 40. Dordrecht, Netherland: Springer; 2014. pp. 445-469

[15] Karsten U, Herburger K, Holzinger A. Living in biological soil crust communities of African deserts-physiological traits of green algal *Klebsormidium* species (Streptophyta) to cope with desiccation, light and temperature gradients. Journal of Plant Physiology. 2016;**194**:2-12

[16] Nishigaki A, Ohshima S, Nakayama K. Characterization of three forms of light-harvesting chlorophyll a/b-protein complexes of photosystem II isolated from the green alga, *Dunaliella salina*. Plant Cell Physiology. 2000;**41**:591-599

[17] Goss R, Wilhelm C, Garab G. Organization of the pigment molecules in the chlorophyll a/b/c containing alga *Mantoniella squamata* (Prasinophyceae)

studied by means of absorption, circular and linear dichroism spectroscopy. Biochimica et Biophysica Acta. 2000;**1457**:190-199

[18] Andreeva A, Stoitchkova K, Busheva M, Apostolova E. Changes in the energy distribution between chlorophyll-protein complexes of thylakoid membranes from pea mutants with modified pigment content: I. changes due to the modified pigment content. Journal of Photochemistry and Photobiology, B: Biology. 2003;**70**:153-162

[19] Foyer CH, Noctor G. Oxygen processing in photosynthesis: Regulation and signaling. New Phytology. 2000;**146**:359-388

[20] Pospíšil P. Production of reactive oxygen species by photosystem II as a response to light and temperature stress. Frontier in Plant Sciences. 2016;**7**:1950

[21] Bowler C, van Montagu M, Inzé D. Superoxide dismutase and stress tolerance. Annual Review of Plant Physiology and Plant Molecular Biology. 1992;**43**:83-116

[22] Clare DA, Rabinowitch HD, Fridovich I. Superoxide dismutase and chilling injury in *Chlorella ellipsoidea*. Archives of Biochemistry and Biophysics. 1984;**231**:158-163

[23] Wolfe-Simon F, Grzebyk D, Schofield O, Falkowski PG. The role and evolution of superoxide dismutases in algae. Journal of Phycology. 2005;**41**:453-465

[24] Ota M, Takenaka M, Sato Y, Lee Smith R, Inomata H. Effects of light intensity and temperature on photoautotrophic growth of a green microalga, *Chlorococcum littorale*. Biotechnology Reports. 2015;**7**:24-29

[25] Terada R, Matsumoto K, Borlongan IA, Watanabe Y, Nishihara GN,

Endo H, et al. The combined effects of PAR and temperature including the chilling-light stress on the photosynthesis of a temperate brown alga, *Sargassum patens* (Fucales), based on field and laboratory measurements. Journal of Applied Phycology. 2018;**30**:1893-1904

[26] Lai CL, Chen TE, Chen JC, Chen PC. Physiological adaptation to dehydration of green alga chlorella sp. strain DT. In: Mathis P, editor. Photosynthesis: From Light to Biosphere. Vol. 4. Dordrecht, Netherland: Kluwer Academic Publishers; 1995. pp. 605-608

[27] Chen PC, Lorenzen H. Changes in productivity and nuclear divisions in synchronous *Chlorella* and circadian rhythm. Plant Cell Physiology. 1987;**27**:1423-1427

[28] Hoffman P, Werner D. Spectrophotometric chlorophyll determination having special regard to various types of equipment. Jena Review. 1966;**7**:300-303

[29] Maxwell K, Johnson GN. Chlorophyll fluorescence — A practical guide. Journal of Experimental Botany. 2000;**51**:659-668

[30] Baker NR. Chlorophyll fluorescence: A probe of photosynthesis in vivo. Annual Review of Plant Biology. 2008;**59**:89-113

[31] Lowry OH, Rosebrough NJ, Farr AL, Randall RJ. Protein measurement with the Folin phenol reagent. Journal of Biological Chemistry. 1951;**193**:265-275

[32] McCord JM, Fridovich I. The utility of superoxide dismutase in studying free radical reactions. I. Radicals generated by the interaction of sulfite, dimethyl sulfoxide, and oxygen. Journal of Biological Chemistry. 1969;**244**:6056-5663

[33] Huang CC, Chen MW, Hsieh JL, Lin WH, Chen PC, Chien LF. Expression of mercuric reductase from *Bacillus megaterium* strain MB1 in eukaryotic microalga *Chlorella sp*. DT: An approach for mercury phytoremediation. Applied Microbiology and Biotechnology. *2006*;**72**:197-205

[34] Fischer BB, Wiesendanger M, Eggen RIL. Growth condition-dependent sensitivity, photodamage and stress response of *Chlamydomonas reinhardtii* exposed to high light conditions. Plant Cell Physiology. 2006;**47**:1135-1145

[35] Gordillo FJL, Jiménez C, Chavarría J, Niell FX. Photosynthetic acclimation to photon irradiance and its relation to chlorophyll fluorescence and carbon assimilation in the halotolerant green alga *Dunaliella viridis*. Photosynthesis Research. 2001;**68**:225-235

[36] Ho TY, Quigg A, Finkel ZV, Milligan AJ, Wyman K, Falkowski PQ, et al. The elemental composition of some marine phytoplankton. Journal of Phycology. 2003;**39**:1145-1159

[37] Darehshouri A, Affenzeller M, Lütz-Meindl U. Cell death upon H_2O_2 induction in the unicellular green alga *Micrasterias*. Plant Biology. 2008;**10**:732-745

[38] Yamazaki JY, Suxuki T, Maruta E, Kamimura Y. The stoichiometry and antenna size of the two photosystems in marine green algae, *Bryopsis maxima* and *Ulva pertusa*, in relation to the light environment of their natural habitat. Journal of Experimental Botany. 2005;**56**:1517-1523

[39] Li T, Huang X, Zhou R, Liu Y, Li B, Nomura C, et al. Differential expression and localization of Mn and Fe superoxide dismutases in the heterocystous cyanobacterim *Anabaena* sp. strain PCC 7120. Journal of Bacteriology. 2002;**184**:5096-5103

[40] Asada K, Kanematsu S, Uchida K. Superoxide dismutases in photosynthetic organisms: Absence of the cuprozinc enzyme in eukaryotic algae. Archives of Biochemistry and Biophysics. 1977;**179**:243-256

[41] Sandnes JM, Kallqvist T, Wenner D, Gislerod HR. Combined influence of light and temperature on growth rates of *Nannochloropsis oceanica*: Linking cellular responses to large-scale biomass production. Journal of Applied Phycology. 2005;**17**:515-525

[42] Atkin OK, Tjoelker MG. Thermal acclimation and the dynamic response of plant respiration to temperature. Trends in Plant Science. 2003;**8**:343-351

[43] Maxwell DP, Falk S, Huner NP. Photosystem II excitation pressure and development of resistance to photoinhibition (I. light-harvesting complex II abundance and zeaxanthin content in *Chlorella vulgaris*). Plant Physiology. 1995;**107**:687-694

[44] Teoh ML, Chu WL, Phang SM. Effect of temperature change on physiology and biochemistry of algae: A review. Malaysia Journal of Science. 2010;**29**:82-97

[45] Hollis L, Ivanov AG, Hüner NPA. *Chlorella vulgaris* integrates photoperiod and chloroplast redox signals in response to growth at high light. Planta. 2019;**249**:1189-1205

[46] Haghjou MM, Shariati M, Smirnoff N. The effect of acute high light and low temperature stresses on the ascorbate-glutathione cycle and superoxide dismutase activity in two *Dunaliella salina* strains. Physiologia Plantarum. 2009;**135**:272-280

[47] Ndong C, Danyluk J, Huner NPA, Sarhan F. Survey of gene expression in winter rye during changes in growth temperature, irradiance or excitation

pressure. Plant Molecular Biology.
2001;**45**:691-703

[48] Janknegt PJ, Rijstenbil JW, van de
Poll WH, Gechev TS, Buma AG.
A comparison of quantitative and
qualitative superoxide dismutase assays
for application to low temperature
microalgae. Journal of Photochemistry
and Photobiology, B: Biology.
2007;**87**:218-226